

Dielectric control of electrostatic barriers for molecular electronics

C. L. Kane and E. J. Mele^{a)}

Department of Physics and Laboratory for Research on the Structure of Matter, University of Pennsylvania, Philadelphia, Pennsylvania 19104

(Received 25 September 2000; accepted for publication 6 November 2000)

We describe an approach for controlling electrostatic barriers in molecular electronics devices which uses anisotropic dielectric material to modify the analytic form of the effective electrostatic interactions within the device. We study the one-dimensional geometry relevant to interfaces between carbon nanotubes and find that the bound charge induced in a uniaxial dielectric can replace the bare electrostatic interaction between charges with separation z by an effective $-\log(z)$ interaction or a *confining* $|z|$ interaction. We use these models to study the depletion region formed at heterojunctions between segments of doped carbon nanotubes. © 2001 American Institute of Physics. [DOI: 10.1063/1.1336162]

Electronic devices formed from bulk semiconductors generally exploit the ability to control the motion of free charge using electrostatic barriers at interfaces between materials. One-dimensional molecular devices are attracting a great deal of attention, but for these systems the reduced dimensionality poses a fundamental difficulty for their operation.^{1,2} This occurs because the Coulomb interaction is a short-range potential in one dimension (its Fourier transform diverges at small momentum q proportional to $-\log q$ instead of $1/q^2$ as in three dimensions). For a p - n junction between segments of doped nanotubes,³ equilibration of the electrochemical potentials at the junction requires either the formation of a very long-range depletion or accumulation region at low doping levels (which can exceed the size of the entire device) or to the formation of an anomalously thin and, therefore, transparent barrier at high doping levels.¹ Importantly, the crossover between these regimes is *exponentially* sensitive to the inverse dopant concentration.

A one-dimensional potential which diverges as $1/q^2$ could avoid this difficulty, but this requires a direct space interaction *proportional* to the separation between charges. Although this cannot be achieved for free charges in vacuum, one can modify the effective interaction between charges for devices embedded in or integrated with various forms of polarizable matter. Here, we show that in a strongly *anisotropic dielectric* one can modify the analytic form of the effective interaction between free charges by controlling the spatial distribution of bound charge induced within the dielectric. In this letter, we analyze three geometries which replace the $1/z$ potential by $-\log(z)$ or $|z|$ potentials, thus permitting the formation of a conventional bandbending profile over length scales useful for submicron device physics.⁴ As an example, we calculate the bandbending profiles for a prototypical p - n junction formed from doped carbon nanotubes including these dielectric effects.

We solve a model geometry in which a nanotube with radius a and axis aligned along the z direction is surrounded by a linear but anisotropic dielectric material characterized by a diagonal susceptibility tensor with $\chi_{zz} \neq \chi_{rr}$. The elec-

trostatic field $E = -\nabla V$ satisfies Gauss' Law $\nabla \cdot E = 4\pi\rho$, where ρ is the total charge density which includes both the free and the bound charges: $\rho = \rho_f + \nabla \cdot \chi \cdot \nabla V$. Within the dielectric $\rho_f = 0$; thus, $(1 + 4\pi\chi_{rr})\nabla_{\perp}^2 V + (1 + 4\pi\chi_{zz})\nabla_{\parallel}^2 V = 0$ and the scalar potential satisfies Laplace's equation in scaled coordinates $(r/\Gamma_{\perp}, z/\Gamma_{\parallel})$, where $\Gamma_{\alpha} = \sqrt{1 + 4\pi\chi_{\alpha}}$. By a suitable choice of the Γ one can, therefore, separately rescale the longitudinal and radial coordinates in the problem.⁵

We now study the total electrostatic potential for this system due to a free-charge distribution on the surface of the cylinder $\sigma_f(\mathbf{r}) = en_q e^{iqz} \delta(r-a)/2\pi a$, where the Fourier amplitude of the number density n_q is dimensionless. The electrostatic potentials for $r < a$ are the Bessel functions of imaginary argument $V_q^<(r) = I_0(qr)$, while in the region $r > a$ we have the solutions $V_q^>(r) = K_0(\Gamma q r)$, where $\Gamma = \Gamma_{\parallel}/\Gamma_{\perp}$. Matching the potential V and radial component of $D = E + 4\pi P$ on the surface of the tube, we find that the electric potential seen on the surface is

$$V_q(r=a) = \frac{2en_q I_0(qa) K_0(\Gamma qa)}{qa[\Gamma I_0(qa) K_0'(\Gamma qa) - I_0'(qa) K_0(\Gamma qa)]}. \quad (1)$$

Equation (1) represents the effective electrostatic interaction between density fluctuations of the free charge on the surface of the cylinder at wave vector q , including the indirect interaction through the polarization of the encapsulating dielectric material.

Figure 1 compares the interaction kernel (1) with the analogous solutions obtained for the cylinder in free space (with $\Gamma = 1$). In both cases, the potential diverges at a small wave vector proportional to $-2 \log(qa/2)$, since at large distances free charges on the surface of the cylinder interact through a $1/z$ potential. At a large wave vector the product $I_0 K_0$ in the numerator decays proportional to $1/q$ and the near-field potential describes the interaction between charged rings $\sim -\log z$. The crossover between these behaviors occurs for momenta $qa \sim 1$, i.e., it occurs at a relatively short range in direct space where the separation between the rings is of the order of the tube radius. When $\Gamma \gg 1$, the anisotropic dielectric effectively rescales the spatial coordinates shifting this crossover to much smaller momenta $\Gamma qa \sim 1$. Thus, the logarithmic form of this potential can be stretched along the

^{a)}Electronic mail: mele@mele.physics.upenn.edu

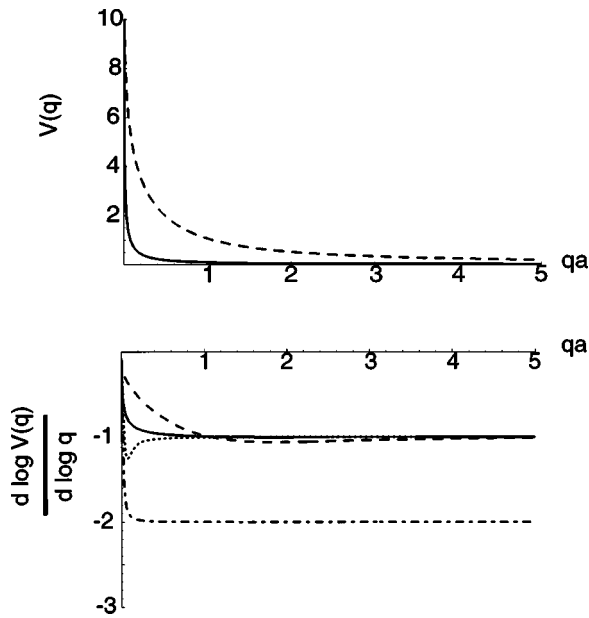


FIG. 1. Fourier transforms of the effective electrostatic interaction between free charges on the surface of the tube in the presence of an anisotropic dielectric. The top panel gives the potential as a function of wave vector q and the bottom panel gives the logarithmic derivative of this potential. The dashed curve is the unscreened potential. The interaction kernels are plotted for an external dielectric (solid), an encapsulated dielectric (dotted), and a dielectric in the tube sidewalls (dot dashed).

axis of the cylinder. The magnitude of this potential is also reduced by a factor of Γ , but this will turn out not to pose a serious difficulty unless Γ is extremely large.

Using the screened electrostatic kernel (1) we compute the bandbending profile near a p - n junction on a nanotube using the self-consistent Thomas-Fermi approach employed in Ref. 1. In this theory, uniformly p - and n -doped cylindrical segments are joined, and the compensating charge densities and electrostatic potentials are computed self-consistently. The *free-charge* distribution is uniformly distributed around the circumference of the cylinder with $n(z) = n_d(z) + n_f(z)$, where n_d is the background dopant density and

$$n_f(z) = \int dE D(E, z) f(E), \quad (2)$$

where $f(E)$ is the Fermi-Dirac distribution function and $D(E, z) = g[E + eV(z)]$ for electrons with charge $-e$ in the presence of the electrostatic potential $V(z)$. Our model for the density of states of a semiconducting tube with gap 2Δ is $g(E) = (4/\pi\hbar v_F) [1 + \Theta(E - \Delta) - \Theta(E + \Delta)]$, where v_F is the Fermi velocity and $\Theta(x) = 1$ for $x > 0$ and zero for $x < 0$.⁶ Figure 2 shows our results for junctions formed from heavily doped tubes with an unscreened interaction $\Gamma = 1$ (dashed curve) and with $\Gamma = 20$ (solid curve). The doping level in these calculations is very large ($n_d \approx 0.02 \text{ \AA}^{-1}$), which leads to a very narrow barrier region and to a high transparency at the contact for the unscreened ($\Gamma = 1$) solution. By contrast, the *screened* solution produces a wide barrier due to the longer range of the effective interaction.

The difference between the screened and unscreened solutions to this problem can be appreciated most clearly by considering the doping dependence of the depletion width, i.e., the region near the junction where the dopants are fully

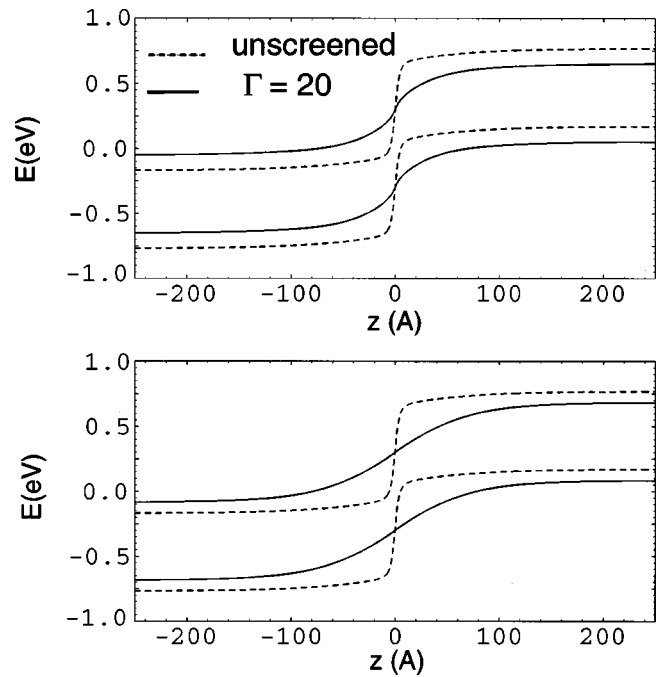


FIG. 2. Bandbending profiles for a p - n junction between heavily doped carbon nanotube segments calculated using the free space (dashed) and screened (solid) interaction kernels for an exterior dielectric (top) and a dielectric incorporated into the tube sidewalls (bottom). The lines denote the locations of the conduction- and valence-band edges as functions of the distance from the junction at $z = 0$. The chemical potential is at $E = 0$.

ionized. Using the unscreened electrostatic kernel, we find that the depletion width scales as $W_u \sim a \exp(\hbar v_F / 6e^2 n_d a)$. By contrast, the *screened* potential varies *logarithmically* with separation over relevant length scales and gives the much more favorable scaling law $W_s \sim \hbar v_F / 6e^2 n_d$.

Remarkably, we find that there is a similar modification to the effective interaction between charges on the tube if the dielectric material is incorporated *inside* the nanotube. Here, the screened interaction kernel, analogous to (1) is

$$V_q(r = a) = \frac{2en_q I_0(\Gamma qa) K_0(qa)}{qa [I_0(\Gamma qa) K'_0(qa) - \Gamma I'_0(\Gamma qa) K_0(qa)]}. \quad (3)$$

The logarithmic derivative of this potential is plotted as the dotted curve in the lower panel of Fig. 1, showing that it also obeys the $1/q$ scaling law in momentum space over a relatively wide range of wave vectors.

The physics that produces this behavior is similar for the exterior and interior problems. The polarization of the exterior or interior anisotropic dielectric produces a volume-bound charge density $-\nabla \cdot \mathbf{P}$ near the tube, as shown in the gray-scale plot of Fig. 3. When $\Gamma \gg 1$, a positive ring of free charge induces a positive plume of bound charge (bright region) that extends along the highly polarizable (z) direction. A compensating negative bound charge (dark region) is found in a shorter-range ring nearer the source charge but also contained within the dielectric. The electric potential seen by a test charge (e.g., an electron) on the surface of the nanotube is the sum of the potentials produced by the unscreened localized source ring on the surface of the tube and the spatially extended bound charges in the dielectric. Thus, the distant test charge sees a near-field potential from the source even if the separation between the source and test

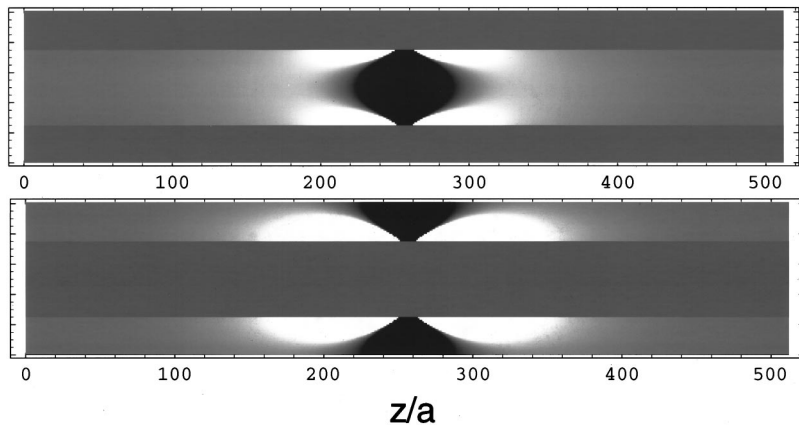


FIG. 3. Cross-sectional view of the bound-charge densities induced in an anisotropic dielectric medium in the presence of a ring of free charge localized on the surface of a nanotube at its center for an encapsulated dielectric (top) and an exterior dielectric (bottom) with $\Gamma=20$. The tube radius is 0.6 nm; for clarity, the heights of the figures are not drawn to scale.

charges span many tube radii. Finally, for a very large separation between source charge and test charge, the test charge ultimately sees *only* the $1/z$ potential produced by the source charge, since the total bound charge is finite in extent and integrates to zero.

A much more dramatic effect occurs in a geometry where the anisotropic material is incorporated into the cylinder sidewalls. We consider a thin-walled cylinder of radius a and thickness w (with $w \ll a$). Here, the electric potential inside and outside the cylinder are the ordinary free-space solutions that are matched by solving the continuum model

$$-\nabla_{\perp}^2 V + [1 + 4\pi\chi_{zz}w\delta(r-a)]q^2V = 2n_q \frac{\delta(r-a)}{a}, \quad (4)$$

which replaces the thin-walled cylinder by a shell of radius a . Solving this boundary value problem we find that the surface potential at $r=a$ is

$$V_q = \frac{2en_q I_0(qa)K_0(qa)}{qa[I_0'(qa)K_0(qa) - I_0(qa)K_0'(qa)] + 4\pi\chi_{zz}waq^2 I_0(qa)K_0(qa)}. \quad (5)$$

The logarithmic derivative of this potential is shown as the dot-dashed line in Fig. 1. For small momenta the second term in the denominator of Eq. (5) vanishes and the potential diverges as $-\log q$, as found in the previous geometries. However, for $4\pi\chi_{zz}waq^2 \gg 1$, one quickly crosses over to a new regime where the second term in the denominator dominates and the effective potential then has the form $V_q \sim en_q/2\pi\chi_{zz}waq^2$. Thus, at short separations in direct space, a point source (here, a localized ring of charge) carries an electric potential that scales as distance from the source proportional to $|z|$, and an electric field on the surface of the tube proportional to $\text{sgn}(z)$. These are properties of an ordinary two-dimensional sheet of charge in a three-dimensional space, and thus this molecular system exhibits the electro-

static properties of an ordinary planar junction. This remarkable behavior ultimately crosses over to the unscreened potential only on the relatively large scale $z_c/a \sim \sqrt{4\pi\chi_{zz}w/a}$. The lower panel of Fig. 2 shows the bandbending profile calculated using Eq. (5), which is nearly identical to the bandbending profile for a planar junction, although here it occurs in low-dimensional geometry.

Implementation of this idea requires the identification of a candidate highly anisotropic material that can be incorporated within the molecular device. One very interesting possibility is that carbon nanotubes themselves, either as single-wall objects packed in a bundle or as multiwalled species, can provide the appropriate material for realizing this effect. It may also be possible to design and control the dielectric anisotropy by embedding short conducting tube segments in a nonconducting matrix. There may be many other routes to the development of nanometer-scale materials with highly anisotropic dielectric properties as well. Materials of this type would be useful for many applications in addition to the ones we have described here.

This work was supported by the DOE under Grant No. DE-FG-02-84ER45118 and by the NSF under Grant No. DMR 98-02560.

¹F. Léonard and J. Tersoff, Phys. Rev. Lett. **83**, 5174 (1999).

²A. A. Odintsov, Phys. Rev. Lett. **85**, 150 (2000).

³L. Chico, V. H. Crespi, L. X. Benedict, S. G. Louie, and M. L. Cohen, Phys. Rev. Lett. **76**, 971 (1996).

⁴Although this method can qualitatively modify the near-field interaction between free charges, the asymptotic long-range potential remains unscreened. This is unavoidable precisely because of the low-dimensional structure of the material but need not prohibit design and fabrication of devices at the nanometer scale.

⁵L. D. Landau and E. M. Lifshitz, *Electrodynamics of Continuous Media* (Elsevier Science, New York, 1960), Sec. 14.

⁶The calculations use $\hbar v_F = 5.41 \text{ eV \AA}$, $\Delta = 0.3 \text{ eV}$, and $a = 6.0 \text{ \AA}$, which are parameters appropriate to a semiconducting single-wall nanotube.